HQSAR Study of Microsomal Prostaglandin E$_2$ Synthase (mPGES-1) Inhibitors

Amor A. San Juan,[†,‡] Seung Joo Cho,[†,*] and Hoon Cho[§,*]

[†]*Biochemicals Research Center, Korea Institute of Science and Technology, Seoul 130-650, Korea.* *E-mail: chosj@kist.re.kr
[‡]*University of Science and Technology, Daejeon 305-330, Korea*
[§]*College of Engineering, Chosun University, Gwangju 501-759, Korea.* *E-mail: hcho@chosun.ac.kr*

Microsomal prostaglandin E$_2$ synthase (mPGES-1) is an enzyme that is associated with inflammation, pain, fever and cancer. Hologram quantitative structure activity relationship (HQSAR) was conducted on the series of MK-886 compounds acting as mPGES-1 inhibitors. A training set with 24 compounds was used to establish the HQSAR model. The best model was chosen based on the cross-validated correlation coefficient ($q^2 = 0.884$) and the correlation coefficient ($r^2 = 0.976$). The model was utilized to predict the activity of the eight-test set of compounds giving the predictive r^2 value of 0.845. The descriptors of the model are based on fragment distinction (atoms, bond and connectivity) and fragment size (2-5 atoms). The atomic contribution maps generated from HQSAR were useful in identifying the important structural features responsible for the inhibitory activity of MK-886 inhibitors. Based on the generated model, the presence of hydrophobic biphenyl group seems to enhance inhibition of mPGES-1 that is in agreement with the previous experiments. In addition, it seems important for a halogen to be substituted to the biphenyl ring and for an acyl group to be attached to the indole moiety for enhanced activity.

Key Words : HQSAR, Drug design, Inflammation, mPGES-1

Introduction

The biosynthesis of prostanoids is regulated by three sequential enzymatic steps[1] such as phospholipase A2 enzymes, cyclooxygenase (COX) enzymes, and various lineage-specific terminal prostanoid synthases. Prostaglandin E synthase (PGES) is present in various forms that isomerize COX-derived PGH2 specifically to PGE2. Two of them are membrane-bound enzymes and have been designated as mPGES-1 and mPGES-2. The microsomal prostaglandin E2 synthase (mPGES-1)[2] is the terminal isomerase in the PGE2 synthetic pathway that is involved in inflammatory response.[3] Specifically targeting mPGES-1 enzyme should interfere almost exclusively with inflammation-induced PGE2, leaving not only the constitutive PGE2 synthesis unaffected, but also the synthesis of other COX-derived prostanoids. Therefore, mPGES-1 inhibition should have more selective effects compared to inhibition of enzymes earlier in the pathway.
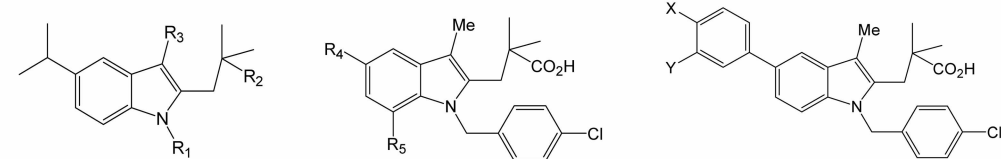
There is an increasing interest to develop an inhibitor that might be selective to PGE2 synthesis by inhibiting mPGES-1, in effect avoiding many of the side effects associated with presently available non-steroidal anti-inflammatory drugs (NSAIDs). Specific removal of PGE2 by inhibition of mPGES-1 may be used to provide the control of inflammatory reactions with fewer side effects in comparison with presently used NSAIDs. To date there are no known specific inhibitors of mPGES-1. A study showed that the N-(2-cyclohexyloxy-4-nitrophenyl)-methanesulfonamide (NS-398) inhibitor (selective cyclooxygenase-2 inhibitor) potently inhibits mPGES-1 activity with an IC$_{50}$ value of 20 μM *in vitro*.[4] Recent research showed that the MK-886 series of inhibitors have promising higher activity for the inducible mPGES-1 membrane protein with the lowest IC$_{50}$ value of 3 nM.[5] The molecular design of potent mPGES-1 inhibitor using MK-886 derivatives might lead the way to the discovery of new anti-inflammatory drugs with few side effects. Moreover, the study will provide additional knowledge in understanding the inhibitory activity of mPGES-1 membrane-bound protein.

Hologram Quantitative Structure Activity Relationship (HQSAR) study is useful to explore the individual atomic contributions to the biological activity. In particular, the atomic contribution maps derived from the HQSAR model were utilized to understand the vital features of the compound's structural fragment corresponding to the biological activity.[5] HQSAR simply utilize information about the atom and bond types from the 2D molecular topology of the various compounds. The significant advantages of HQSAR technique in studying the quantitative structure-activity relationships of mPGES-1 inhibitors include no requirement for 3D structure of the compounds, shorter computation time, simple reproducibility, convenience and the visual color codes of atomic contribution maps. In this study, HQSAR analysis was employed to MK-886 series of inhibitors reported by Riendeau *et al.*[6]

Methods

Data set. The compounds used for the HQSAR analysis include MK-886 derivatives obtained from a report published by Riendeau *et al.*[6] The report consists of 32 compounds with IC$_{50}$ values in the range of 0.003 to 10 μM (see Table 1) by which both of the training and test set compounds were

Table 1. The binding affinity of MK-886 derivatives (Riendeau *et al.* [6])

substituted MK-886 for compounds **1-14**

substituted indoles for compounds **15-19**

substituted 5-phenyl indoles for compounds **20-32**

Compound	R_1	R_2	R_3	R_4	R_5	X	Y	IC_{50} (uM)
1	$CH_2(4\text{-}Cl\text{-}Ph)$	CO_2H	S^tBu					1.600
2	H	CO_2H	S^tBu					10
3	Me	CO_2H	S^tBu					10
4	$CH_2(CH=CH_2)$	CO_2H	S^tBu					6.700
5	$(CH_2)_3Ph$	CO_2H	S^tBu					3.200
6	$CH_2(4\text{-}Cl\text{-}Ph)$	CO_2Me	S^tBu					7.200
7	$CH_2(4\text{-}Cl\text{-}Ph)$	$CONH_2$	S^tBu					10
8	$CH_2(4\text{-}Cl\text{-}Ph)$	CO_2H	Ph					6.400
9	$CH_2(4\text{-}Cl\text{-}Ph)$	CO_2H	O Ph					0.650
10	$CH_2(4\text{-}Cl\text{-}Ph)$	CO_2H	$CH_2(4\text{-}^tBu\text{-}Ph)$					0.290
11	$CH_2(4\text{-}Cl\text{-}Ph)$	CO_2H	$CO(2\text{-}Me\text{-}Ph)$					0.900
12	$CH_2(4\text{-}Cl\text{-}Ph)$	CO_2H	$COCH_2S^tBu$					0.260
13	$CH_2(4\text{-}Cl\text{-}Ph)$	CO_2H	$COCH_2^tBu$					0.250
14	$CH_2(4\text{-}Cl\text{-}Ph)$	CO_2H	Me					1.100
15				H	^iPr			4.300
16				H	H			3.200
17				F	H			2.600
18				^tBu	H			0.330
19				Ph	H			0.600
20						Ph	H	0.160
21						H	Ph	0.016
22						Cl	Ph	0.022
23						F	Ph	0.007
24						F	5-(1,3-pyrazinyl)	0.032
25						F	3-pyridinyl	0.012
26						F	2-MeO-Ph	0.005
27						F	2-Cl-Ph	0.004
28						F	2-F-Ph	0.008
29						F	2-MeCO-Ph	0.006
30						F	2-Me-Ph	0.003
31						F	2-Me-Ph	0.033
32						F	2-Me-Ph	0.031

chosen. The training set of compounds were used to derive the model whereas, the test set of compounds were used to determine the predictability of the model. From these 32 compounds, only 24 compounds were selected as training set and 8 compounds (1, 7, 9, 16, 20, 24, 26 and 31) were taken as test set. The IC_{50} values of the training set were converted into pIC_{50} (-$\log IC_{50}$) and subsequently used as dependent variables in the HQSAR analysis. The most potent compound from the series which is 3-[1-(4-chloro-benzyl)-5-(2-fluoro-2'-methyl-biphenyl-4-yl)-1H-indol-2-yl]-2,2-dimethyl-propionic acid (see Figure 1) shows that the biaryl rings (A and B) yields the remarkable potency of the compound based on *in vitro* biochemical assay.[6]

Molecular modeling by HQSAR. Hologram QSAR (HQSAR) is a recently developed molecular modeling package.[5] The basis of HQSAR is from the concept of unity

hashed binary bit strings called fingerprint[7] that employs structural fragment to predict the activity of a potent compound. Molecular 2D-fingerprints had been a very popular tool in analyzing chemical similarity. In HQSAR molecular fragment, the 2D-fingerprint is employed in predicting the biological activity of compounds. Particularly, HQSAR uses molecular hologram as an extended 2D-fingerprint that encodes elaborate structural information including stereochemistry as well as branched and cyclic molecular fragments. HQSAR[8] is a robust technique that is fast, reliable and does not require alignment of compounds.

Molecular modeling calculations by HQSAR were performed using SYBYL[9] program version 7.1 on Silicon graphics origin300 workstation with IRIX 6.5 operating system. In HQSAR approach, the initial step undertaken was the generation of molecular holograms from the structure of
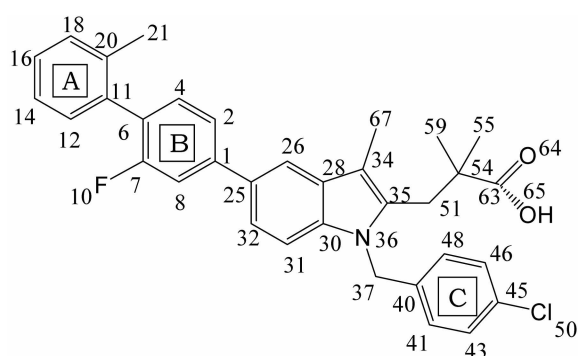
Figure 1. The two-dimensional chemical structure of the model compound.

compound, followed by correlation through statistical PLS analysis. Molecular holograms were obtained by breaking down molecular structures into all possible linear and branched fragments of connected atoms. The 2D-finger-prints of the compounds were generated for all the sub-structures with topological descriptors based on fragment distinction (atoms, bond and connectivity) and fragment size (2-5 atoms). Each unique fragment in a data set was then assigned a specific large positive integer by means of a cyclic redundancy check algorithm. Each of these integers corresponds to a bin in an integer array of 53, 59, 61, 71, 97, 151, 199, 275, 307, 353, 401, and 997 as fixed prime number hologram lengths. The computation of molecular holograms for a dataset of structures generates data matrix with a dimension of R x L. The R represents the number of com-pounds in the training set while L represents the length of the molecular hologram. Subsequently, after the molecular holograms were created, the statistical calculations were employed to finally generate a model inhibitor.

Statistical calculations. Partial least squares (PLS) methodology[10,11] was employed to determine the relation-ship between the 2D-fingerprint and biological activity of the compounds. To derive a HQSAR model, the structural features of the descriptors were used as independent variables and the pIC₅₀ values were utilized as dependent variables in PLS analyses. Initially, the predictive value of the model was determined by leave-one-out (LOO)[12] cross-validation. The results from the LOO calculation were utilized to obtain the number of components that yield an optimally predictive model. Based on the generated model, the final calculation of the activity of compounds is represented by the mathematical equation below. The equation relates the values of molecular hologram bins to the corresponding biological activity in each of the compounds in the training set.

$$\text{Activity}_i = c_o + \Sigma_L c_{il} x_{il}$$

The representations of the abbreviations in the equation are: Activity$_i$ represents the biological activity of the compound, c_o is a constant, L is the hologram length, c_{il} is the coefficient for the bin derived from the PLS analysis, and x_{il} is the occupancy value of the molecular hologram of compound i at position or bin l.

HQSAR contribution maps. The graphical displays of the HQSAR computational analysis were shown by color-coded structure diagram representing the degree of contri-bution of atoms in linearity with its activity. Poor atomic contributions were represented by the colors red, red-orange and orange that are located at the red end of the color spectrum. Favorable atomic contributions were represented by the colors yellow, green-blue and green that are located at the green end of the color spectrum. On the other hand, intermediate atomic contributions were exhibited in color white. By default, HQSAR specifies the maximal common structure (MCS) based on the similar backbone present in all of the compounds from the training set. MCS is denoted by color cyan. It should be noted that the contribution to activity of the atoms involved in MCS were ignored since the template is common to all structures and thus, does not provide a distinguishing feature among the compounds in the dataset.

Predictive R squared (r^2_{pred}). To validate the derived model from HQSAR, the biological activities of the eight-test set of compounds were predicted using the model generated from the training set. The predictive ability of the model is expressed by predictive r^2 value, which is similar to cross-validated r^2 (q^2) and is calculated by using the formula below:

$$r^2_{pred} = \frac{SD - PRESS}{SD}$$

wherein, SD is the sum of the squared deviation between the biological activities of the test set compounds and the mean activity of the training set compounds and PRESS is the sum of the squared deviations between the observed and the predicted activities of the test set compounds.

Results and Discussion

A set of factors such as fragment size, number of frag-ments, atom types (A), bond types (B), atom hybridization or connectivity (C), hydrogen bond and donor (H), were modified to search the best cross-validation r^2 of the model. The fragment parameters including A, B, C and H were user-selectable flags that provided rules to determine the type of unique structural features of the model compound. Atom flag provides the ability to differentiate between fragments based on differences in element types. Bond flag distinguishes between fragments based on differences in bond types. Connection flag allows the distinction of hybridization state of the atoms in the fragment. Hydrogen flag distinguishes whether or not hydrogen atoms are included in the fragment.

In the initial HQSAR analysis, the default fragment size of 4-7 atoms was employed for the different combinations of fragment distinction (see Table 2) parameters including atom types (A), bond types, (B), connectivity (C), and hydrogen (H). Next, the best hologram length (L) and optimum number of components (N) were selected based on the PLS analysis that gave the least cross-validated standard error

1534 *Bull. Korean Chem. Soc.* **2006**, Vol. 27, No. 10

Amor A. San Juan et al.

Table 2. HQSAR analysis for various fragment distinction using fragment size (4-7)

Fragment distinction	q^2	SE_{CV}	r^2	SE	N	Length
A	0.783	0.576	0.894	0.403	3	353
B	0.767	0.571	0.799	0.530	1	199
C	0.816	0.573	0.982	0.179	6	353
AB	0.795	0.547	0.860	0.452	2	257
AC	0.788	0.557	0.864	0.446	2	151
BC	0.861	0.472	0.983	0.165	4	353
ABC	0.870	0.457	0.986	0.149	4	307
AH	0.824	0.546	0.946	0.304	5	199
BH	0.739	0.617	0.798	0.543	2	353
CH	0.773	0.575	0.832	0.495	2	307
ABH	0.810	0.582	0.971	0.229	6	353
ACH	0.819	0.539	0.928	0.340	4	151
BCH	0.818	0.556	0.939	0.321	5	151
ABCH	0.847	0.523	0.968	0.240	6	151

q^2 –LOO cross-validated correlation coefficient, SE_{CV} –cross-validated standard error. r^2 –noncross-validated correlation coefficient, SE – noncross-validated standard error. N –number of components, Length – hologram length. *Fragment distinction:* A –atom types, B –bond types, C –connectivity, H –hydrogen.

Table 3. HQSAR analysis for the influence of various fragment sizes using the best *fragment distinction* (A/B/C)

Fragment size	q^2	SE_{CV}	r^2	SE	N	Length
2 – 5	0.884	0.431	0.976	0.196	4	97
3 – 6	0.875	0.448	0.977	0.194	4	97
4 – 7	0.870	0.457	0.986	0.149	4	307
5 – 8	0.864	0.468	0.979	0.183	4	307
6 – 9	0.867	0.474	0.982	0.173	5	151
7 – 10	0.818	0.516	0.905	0.372	2	307

q^2 –LOO cross-validated correlation coefficient, SE_{CV} –cross-validated standard error. r^2 –noncross-validated correlation coefficient, SE – noncross-validated standard error. N –number of components, Length – hologram length.

(SE$_{CV}$). The PLS analysis was repeated by employing different fragment sizes (see Table 3) using the best fragment distinction obtained from the previous step. Finally, a HQSAR model (hologram) was derived from the training set.

HQSAR model. A total of 24 structurally similar indoles served as training set to establish the model. The best HQSAR model was generated (descriptors: atoms, connections, bonds; fragment length: 2-5, hologram length: 97). The best model taken from the results of PLS analysis in the training set yielded (see Table 4) a cross-validated q^2 value of 0.884 with four optimal components, and non-cross validated r^2 value of 0.976 with a standard error of 0.431. The selected model was validated by a test set of 8 compounds (shown as bold in Table 5), giving satisfactory predictive r^2 value of 0.845. Based on the HQSAR model, the relationship between the experimental and predicted activities of both the training and test set were fairly

Table 4. Statistical indexes of HQSAR model

Dataset	q^2	SE_{CV}	r^2	SE	N	Length
Training	0.884	0.431	0.976	0.196	4	97
Test	0.901	0.462	0.943	0.351	1	151

q^2 –LOO cross-validated correlation coefficient, SE_{CV} –cross-validated standard error. r^2 – noncross-validated correlation coefficient, SE – noncross-validated standard error. N –number of components, Length –hologram length.

Table 5. Relationship between experimental and predicted activities

Compound	Experimental p$IC50$	Predicted p$IC50$	Residual
Training			
2	–1.04	–1.06	–0.02
3	–1.04	–0.96	0.08
4	–0.83	–0.81	0.02
5	–0.51	–0.61	–0.10
6	–0.86	–0.82	0.04
8	–0.81	–0.76	0.05
10	0.54	0.53	–0.01
11	0.05	–0.09	–0.14
12	0.58	0.65	0.07
13	0.60	0.69	0.09
14	–0.04	–0.03	0.01
15	–0.04	–0.03	0.01
17	–0.51	–0.65	–0.14
18	–0.41	–0.39	0.02
19	0.48	0.54	0.06
21	0.80	1.30	0.50
22	1.80	1.30	–0.50
23	1.66	1.79	0.13
25	1.50	1.36	–0.14
27	2.30	2.07	–0.23
28	2.40	2.23	–0.17
29	2.10	2.14	0.04
30	2.22	2.20	–0.02
32	1.48	1.68	0.20
Test			
1	–0.20	–0.57	–0.37
7	–1.04	–0.74	0.30
9	0.19	–0.16	–0.35
16	–0.63	0.16	0.79
20	0.22	0.28	0.06
24	2.15	1.72	–0.43
26	1.92	1.55	–0.37
31	2.52	1.67	–0.85

predicted with residual values less than one log unit (see Table 5). In Figure 2, the graph represents the correlation between the experimental and predicted activities for both the training and test set of compounds.

Atomic contribution maps. The various colors of each atom reflect the degree of contribution towards the overall activity of the compound. The colors reflecting poor (or negative) contributions are at the red end of the spectrum (red, red orange, and orange), while the colors reflecting favorable (positive) contributions are at the green end (yellow, green blue, and blue). Atoms colored in white
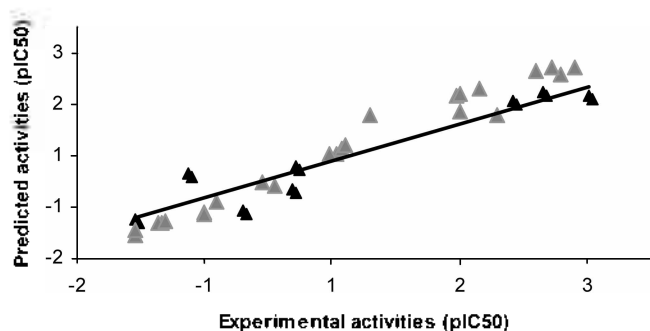
Figure 2. The plot of experimental and predicted activities (r^2 = 0.9414) for series of MK-886 inhibitors. The bold triangle denotes training set while the gray triangle represents test set.

reflect intermediate contributions.

In atomic contributions, the min_contrib and max_contrib denote the minimum and maximum PLS coefficients related to the biological activity respectively, the colors used are:

	red	<5/6min contrib
5/6min contrib<	red orange	<1/2min contrib
1/2min contrib<	orange	<1/3min contrib
1/3min contrib<	white	<1/3max contrib
1/3max contrib<	yellow	<1/2max contrib
1/2max contrib<	green blue	<5/6max contrib
5/6max contrib<	green	

For the system discussed in this work, the values of min_contrib and max_contrib were provided after the construction of HQSAR model and the colors reflect the contributions *as below*:

	red	<−0.0526825
−0.0526825<	red orange	<−0.0316095
−0.0316095<	orange	<−0.0210730
−0.0210730<	white	< 0.11352467
0.11352467<	yellow	< 0.170287
0.170287<	green blue	< 0.2881167
0.2881167<	green	

Figure 3 depicts the individual atomic contribution of the model compound to its molecular bioactivity. It indicates that the hydrophobic biphenyl group mainly contributes the overall activity of the compound. The condensed rings A and B (refer to Figure 1) were colored green and yellow (see Figure 3) which indicates positive contribution to the activity, suggesting that this is a pharmacologically important group. The particular atoms of the biphenyl ring with positive contributions to activity include C_2, C_4, C_6, C_7, C_{11}, C_{12}, C_{14}, Cl_{50} and F_{10}. The importance of the hydrophobic group (biphenyl) attached to the indole ring is supported by the contribution map of other compounds (see Figures 4-5). In Figure 4, the contribution map marked a moderate activity
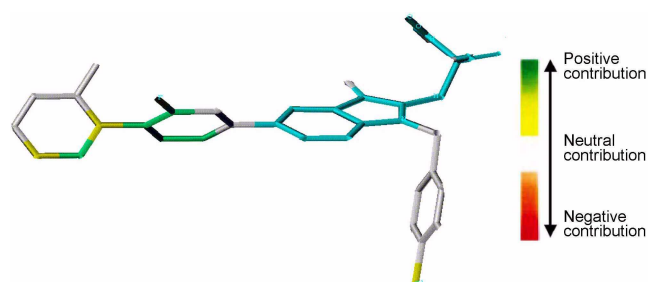

Figure 3. The atomic contribution map for the most potent inhibitor to mPGES-1. Green and yellow colors imply highest to higher atomic contributions to the activity, respectively. The atoms with intermediate contributions are colored white while cyan color denotes the backbone structure.
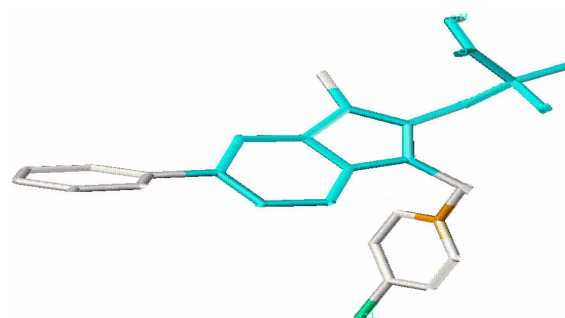

Figure 4. The intermediate contribution (white color) of the B-phenyl ring (refer to Figure 1) to mPGES-1 activity.

(white color) from a single phenyl group attached to the backbone structure indole (cyan). In Figure 5, the addition of another phenyl moiety to the existing benzene ring attached to the backbone indole indicated a high positive contribution to activity. When a 3-pyridinyl group was attached into the A-phenyl group (see Figures 1 and 6), the color of the atomic contribution map has changed from green color (favorable activity) into white color (moderate activity). The addition of fluorine atom substituent to the B-phenyl ring (refer to Figure 1) suggested an enhance activity of the compound (see Figure 7). For further bioactivity improvement, the modification of atoms at C ring (refer to Figure 1) with color white (see Figure 3) might enhance activity. In Figure 8, the presence of acyl substituent ($COCH_2S^tBu$) yield favorable activity that implies this moiety should be maintained for future SAR studies.
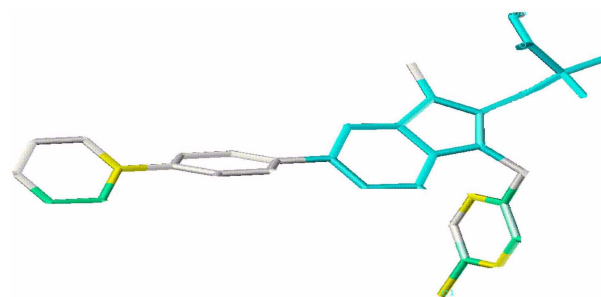

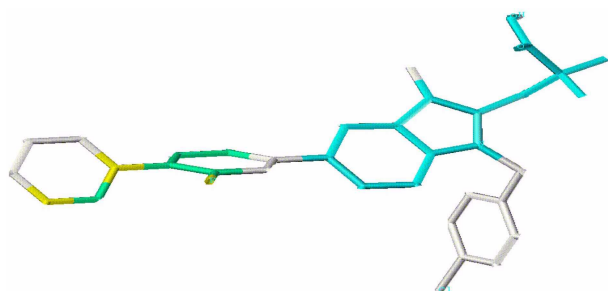**Figure 5.** The enhancement to mPGES-1 activity by the presence of A-phenyl ring (refer to Figure 1).

Figure 6. The intermediate activity of 3-pyridinyl attached to the B-phenyl ring (refer to Figure 1).
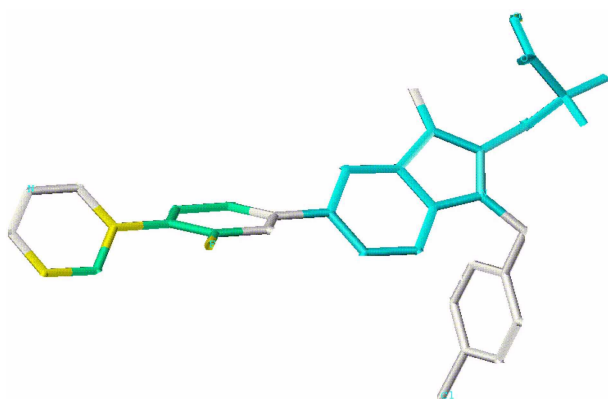

Figure 7. The positive contribution of electronegative fluorine atom attached to the B-phenyl ring (refer to Figure 1).
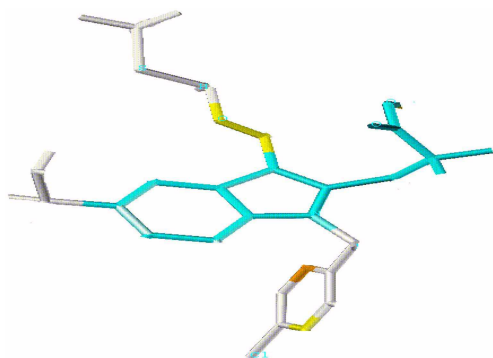

Figure 8. The positive contribution of acyl substituent (yellow color) to mPGES-1 activity.

Validation of the HQSAR model using test set. To verify predictability of the constructed HQSAR model based on the training set, 8 compounds were selected as testing set for validation. The predicted bioactivities of the test set were shown in Table 5. The correlation between the predicted and experimental results was depicted in Figure 2 (shown in bold triangles). The PLS analysis on the test set released cross-validated q^2 value of 0.901 and r^2 value of 0.943 with a standard error of 0.462. In addition, the predictive r^2 value of 0.845 may suggests a satisfactory model. All of the statistical results demonstrate that the HQSAR model is fairly reliable with good predictive ability and could be helpful in discovering new drugs for inflammation.

Conclusion

The HQSAR study provides display of color codes to reflect which molecular fragments of the compound may be important contributors to the biological activity. The result indicates that the biphenyl ring and its substituent are the particular types of atoms that contribute to the overall activity of the model compound, in agreement with the previous experiment.[6] The importance of hydrophobic biphenyl moiety with favorable activity is exemplified by further results of contribution maps. First, by attaching a monophenyl instead of biphenyl moiety to the core indole has indicated an intermediate contribution to activity. Second, the attachment of 3-pyridinyl to A-phenyl moiety implied a lesser activity. On the other hand, the attachment of an acyl substituent to the 3-indolyl moiety of the model might enhance the activity. Based on the overall results, it seems reasonable to consider the relevance of the hydrophobic biphenyl group in mPGES-1 activity. The hydrophobic group enhances mPGES-1 inhibition that is in agreement with the report[13] of fatty acid analogues as mPGES-1 inhibitors. In addition, the results suggest the halogen substitution to the biphenyl ring and the attachment of an acyl substituent to the indole moiety would favor activity to mPGES-1.

References

1. Kudo, I.; Murakami, M.; Prostaglandin, E. *J. Biochem. Mol. Biol.* **2005**, *38*(6), 633-638.
2. Shinji, Y.; Tsukui, T.; Tatsuguchi, A.; Shinoki, K.; Kusunoki, M.; Suzuki, K.; Hiratsuka, T.; Wada, K.; Futagami, S.; Miyake, K.; Gudis, K.; Sakamoto, C. *Am. J. Physiol. Gastrointest Liver Physiol.* **2005**, *288*, G308-G315.
3. Ek, M.; Engblom, D.; Saha, S.; Blomqvist, A.; Jakobsson, P.; Ericsson-Dahlstrand, A. *Nature* **2001**, *410*, 430-443.
4. Thoren, S.; Jakobsson, P. J. *Eur. J. Biochem.* **2000**, *267*, 6428-6434.
5. Lowis, D. R. *Tripos Technical Notes* **1997**, *1*, 1-16.
6. Riendeau, D.; Aspiotis, R.; Ethier, D.; Gareau, Y.; Grimm, E.; Guay, J.; Guiral, S.; Juteau, H.; Mancini, J.; Methot, N.; Rubin, J.; Friesen, R. *Bioorg. Med. Chem. Lett.* **2005**, *15*, 3352-3355.
7. Flower, D. *J. Chem. Inf. Comput. Sci.* **1997**, *38*(3), 379-386.
8. Cho, S. J. *Bull. Korean Chem. Soc.* **2005**, *26*(1), 85-90.
9. *SYBYL 7.0*; Tripos Inc.: St. Louis, 2004.
10. Cramer, R. D. III; Bunce, J. D.; Patterson, D. E. *Quant. Struct. Act. Relat.* **1998**, *7*, 18-25.
11. Wold, S.; Albano, C.; Dunn, W.; Edlund, U.; Esbensen, K.; Geladi, P.; Hellberg, S.; Johansson, E.; Lindberg, W.; Sjosstrom, M. In *Chemometrics: Mathematics and Statistics in Chemistry*; Kowalski, B., Ed.; Reidel, Dordrecht, The Netherlands, 1987; pp 17-95.
12. Bush, B. L.; Nachbar, R. B. *J. Comput. Aided Mol. Des.* **1993**, *7*, 587-619.
13. Quraishi, O.; Mancini, J.; Rindeau, D. *Biochem. Pharma.* **2002**, *63*, 1183-1189.